Available online at www.sciencedirect.com
SCIENCE DIRECT®
Journal of Photochemistry and Photobiology A: Chemistry 161 (2004) 233–242
Journal of Photochemistry and Photobiology A:Chemistry
www.elsevier.com/locate/jphotochem

Photoelectrocatalytic degradation of quinoline with a novel three-dimensional electrode-packed bed photocatalytic reactor

Taicheng An[a,*], Wenbing Zhang[a], Xianming Xiao[a], Guoying Sheng[a], Jiamo Fu[a], Xihai Zhu[b]

[a] *State Key Laboratory of Organic Geochemistry, Guangdong Key Laboratory of Environmental Resources Utilization and Protection, Guangzhou Institute of Geochemistry, Chinese Academy of Sciences, Guangzhou 510640, PR China*
[b] *School of Chemistry and Chemical Engineering, Zhongshan University, Guangzhou 510275, PR China*

Received 8 June 2003; received in revised form 21 July 2003; accepted 2 August 2003

Abstract

Photoelectrocatalytic degradation performance of quinoline in saline water was assessed with a newly designed continuous flow three-dimensional electrode-packed bed photocatalytic reactor. The efficiency of the three-dimensional electrode electrochemically assisted photocatalytic process was measured in terms of degradation and mineralization of quinoline. It was found that quinoline could be degraded more efficiently by photoelectrochemical process than by photocatalytic or electrochemical oxidation in saline water. The experimental results showed that oxidation of quinoline by photoelectrochemical process were well described with a pseudo first-order kinetics. The dependence of the rate constants on various parameters in the photoelectrocatalytic reactor, such as initial concentration of chloride ion, applied cell voltage, airflow and pH value were investigated in detail. Photoelectrocatalytic degradation of quinoline was more favorable in alkali solution than in acidic solution. It is also interesting to note that chloride ion had an obvious enhancement effect rather than a scavenging effect on the photoelectrocatalytic degradation of quinoline in saline water. A kinetic synergetic effect was observed with an enhancement of the rate constant by a factor of 3.7 compared to photoelectrocatalytic degradation of quinoline without addition of Cl^- ion.

Keywords: Photoelectrocatalytic; Packed bed reactor; Photocatalytic enhancement; Synergetic effect; Chloride ion; Quinoline

1. Introduction

In spite of numerous approved patents related to heterogeneous photocatalysis, the development of practical water treatment systems have not yet been successfully achieved because of high degree of recombination of photogenerated electron and hole [1]. Thus, it is of great interest to improve the photocatalytic activity of semiconductors for degradation of organic compounds in water and air. Recently, several studies attempted to increase the photocatalytic efficiency of titanium dioxide, by using techniques such as noble metal deposition [2,3], ion doping [4] and coupled semiconductor oxide [5,6]. Alternatively, photoelectrocatalysis is considered to be a better approach, because the problem of high degree charges recombination presented in heterogeneous photocatalysis can be solved successfully by applying an anodic bias [7–13]. Recent studies have repeatedly confirmed that the external electric field could greatly enhance photocatalytic efficiency, which is well known as an electric field enhancement effect [14–16]. However, in most of electrochemically assisted photocatalytic experiments [14–16], the applied anodic bias potentials were lower than the oxidation potential of objective organic pollutant so that no direct electrochemical oxidation interferes with the photocatalysis. Actually, it is worth pointing out that electrochemistry is also an effective method for degrading organic pollutants under high external electric field. In particular, the electrochemical technology based on three-dimensional electrode has attracted much attention recently [17,18] because the three-dimensional electrode technology is characterized by large specific surface areas and high performance in comparison to conventional two-dimensional plate electrode [17,19]. However, only a few reports have discussed this hybrid photoelectrochemical technology under higher electric fields, which combines photocatalysis with the three-dimensional electrode technology [20–22].

Effects of various inorganic ions on TiO_2 slurry catalyst and fixed-bed catalyst systems were reviewed by Burns et al. [23] who concluded that all inorganic compounds including sodium chloride were found to inhibit photocatalysis at

* Corresponding author. Tel.: +86-20-8529-1501; fax: +86-20-8529-0706.
E-mail address: antc99@gig.ac.cn (T. An).

1010-6030/$ – see front matter © 2004 Elsevier B.V. All rights reserved.
doi:10.1016/j.nainr.2003.08.004

all the concentrations tested. A few studies have been conducted to investigate the effects of chloride ions on the photoelectrocatalytic degradation of organic contaminants [7,24]. Candal et al. [7] found that when potentials were applied across the titania coatings the photoelectrocatalytic activities were not inhibited significantly in the presence of sodium chloride. But, with respect to photoelectrochemical process, chloride ion may be a scavenger of $^{\bullet}OH$ radical or a poisonous reagent to photocatalyst, but also a supporting electrolyte for electrochemical process. Up to date, there have been very few systematic studies investigating the effect of chloride ions on photoelectrocatalytic process. Thus, it is of interest to elucidate how chloride ions influence the photoelectrocatalytic process. In a previous study, we found that the external electric field depressed the deactivation of TiO_2 photocatalyst in the presence of high concentrations of Cl^- ions [25]. The photoelectrocatalytic efficiency of HCOOH decreased initially then increased rapidly with increasing Cl^- ion concentrations in the slurry photoelectrocatalytic reactor. However, all of these efficiencies were lower than that obtained in the photocatalytic process without addition of Cl^- ions. To date, all researchers did not find any enhancement effect at all tested concentration of Cl^- ions.

More recently, our research group has successfully combined the slurry photocatalytic oxidation technology with the plate electrodes and three-dimensional electrodes, respectively, to develop two photoelectrocatalytic reactors, slurry photoelectrocatalytic reactor [20] and three-dimensional electrode-slurry photocatalytic reactor [21,22] for the degradation of pollutants in water. In the present study, a novel continuous flow three-dimensional electrode-packed bed photocatalytic reactor was developed, which is an improved version over two photoelectrocatalytic reactors, reported previously in literatures [20–22], and quinoline was used as a model compound to investigate the degradation of the organics in saline water.

2. Experimental

2.1. Materials

Quinoline (98%) of analytic grade was purchased from Sigma and prepared with deionized water at the concentration of 0.25 mmol l^{-1}. NaCl was used as supporting electrolyte in the photoelectrocatalytic process at the concentration of 0.5 mol l^{-1}. Titanium dioxide Degussa P25 is composed mainly of anatase (ca. 70%), having the shape of non-porous polyhedral particles with a mean size of ca. 30 nm and a surface area of 50 $m^2\,g^{-1}$. Analytic grade quartz sand with particulate diameters of 2–4 mm was used as the supports of photocatalyst. The material of quartz sand coated by TiO_2 was used as the filler both for the three-dimensional electrode and for the packed bed photocatalyst in this photoelectrocatalytic reactor. The micropore titanium plate was used as electrodes after dealt with diluted sulfuric acid and then washed with deionized water twice. All other reagents were analytic grade.

2.2. Preparation of quartz sand-supported TiO_2

A 200-ml aqueous suspension containing 5 g of TiO_2 was agitated for 4 h and sonicated for 30 min, and then used for coating quartz sand. Upon cleanup by sonication in deionzed water, 500 g of quartz sand were immerged in the suspension solution for 30 min. The mixture was dried at 120 °C and then calcined for 4 h in an oven at 450 °C. Loading, drying and calcining were repeated twice. After being washed with deionzed water, the material was dried at 120 °C and weighed. The quantity of TiO_2 coating on quartz sand was about 0.0182 g g^{-1}. The SEM micrographs of the coated material were obtained by a LEO1530VP microscope (LEO, Germany), and a typical micrograph was presented in Fig. 1. It can be seen from the micrograph that TiO_2 was distributed uniformly on the supports, and the average size was exactly the same as the original size of Degussa P25 TiO_2.

2.3. Photoelectrocatalytic reactor

The set-up is a continuous flow three-dimensional electrode-packed bed photocatalytic reactor. The reactor was based on the three-dimensional electrode-slurry photocatalytic reactor [21,22] and the slurry photoelectrocatalytic reactor [20] as reported in our previous research works. The reaction setup is consisted of 250-ml flow-through photoelectrocatalytic reactor connected to a 500 ml reservoir. As shown in Fig. 2, it is consisted of an outer cylindrical Pyrex casing (i.d. = 60 mm; height = 300 mm) fitted with a gas distributor (porous titanium plate with a pore size of less than 40 μm) and a PVC base. A 500 W high-pressure mercury lamp was suspended vertically in a double-wall U-tube through which 5.0 mm-thick cooling water flows (800 ml min^{-1}) to maintain reaction isothermality. The quartz sand-supported TiO_2 was packed between the annulus of the inside quartz U-tube and the outer Pyrex cylinder, and the thickness of the supports was 5.0 mm. The packed material was used both for the photocatalyst of packed bed photocatalytic reactor and for the particle electrode of the three-dimensional electrode electrochemical reactor. That is, the photoelectrocatalytic reactor is a couple of a packed bed photocatalytic reactor with a three-dimensional electrode electrochemical reactor. Compressed air was bubbled upward through the gas distributor equipped at the bottom of the reactor. It is also worth mentioning that the porous titanium plate was used not only as a gas distributor but also as an anode in this reactor, different from all the photoelectrochemical reactors reported previously. At the same time, the cathode is also a cirque made of porous titanium plate, located about 15 cm above the anode. External cell voltage was controlled by a WYK-305 potentiostat (Yangzhou, China). The reaction solution was recirculated through the

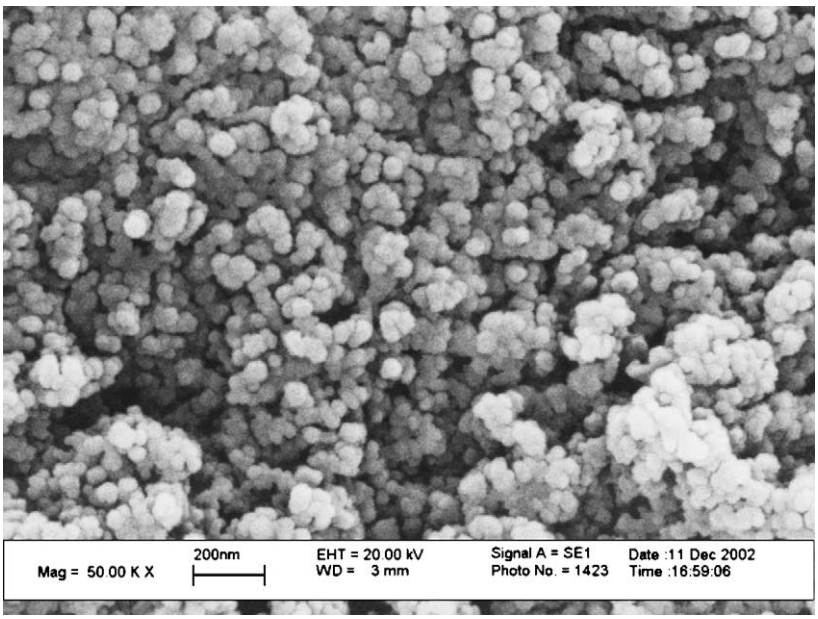

Fig. 1. A typical SEM micrograph of the quartz sand-supported TiO_2.

system at a flow rate of ca. 190 ml min^{-1} using a peristaltic pump. Additionally, the exterior wall of the reactor was covered with a reflecting aluminum foil to improve the efficiency of UV utilization.

2.4. Analysis

Progress of all reactions was monitored by HPLC. Millpore membrane (0.45 μm) was used to remove solid mass of the colloid solution before the HPLC analysis. Analysis was achieved by a Hewlett Packard 1100 system equipped with an UV-Vis detector and a reverse phase C_{18} column (Dikma, 250 mm × 4.6 mm i.d.). The column was eluted with a mixture of water–methanol 40:60 v/v with a flow rate of 1.0 ml min^{-1}. 5 μl filtered sample was injected into HPLC system and the detection was performed by UV absorption at 225 nm. The total organic carbon reduction was measured with a Phoenix 8000 TOC analyzer.

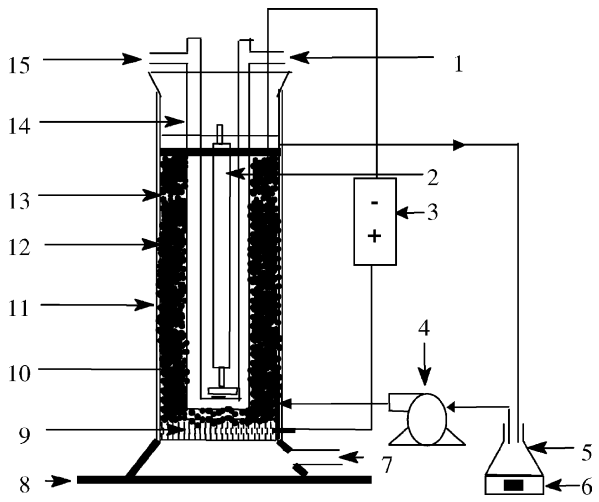

Fig. 2. Schematic diagram of reactor setup: (1) inlet of recycled water; (2) high-pressure mercury lamp; (3) potentiostat; (4) pump; (5) reservoir, (6) magnetic stirrer, (7) inlet of compressed air; (8) base of reactor; (9) micropore titanium plate anode; (10) Packed material; (11) aluminum foil; (12) outer Pyrex cylinder; (13) a porous titanium cirque cathode; (14) double-welled quartz U-tube; (15) outlet of recycled water.

2.5. Experimental procedures

A 500 ml solution of quinoline containing 0.5 mol l^{-1} NaCl was used to conduct the experiment. A peristaltic pump at the flow of 190 ml min^{-1} pumped the solution through the photoelectrochemical reactor, and the residual solution was well stirred by a magnetic stirrer. The reaction was started when the d. c. power, illumination and compressed air supply were switched on. Except as indicated, general treating conditions were 30 V direct current cell voltage, 0.05 MPa airflow, 0.25 mmol l^{-1} quinoline, natural pH value and 0.5 mol l^{-1} NaCl solution. Once the experiment was started, samples were withdrawn from the reservoir at desired intervals for the analyses of quinoline and the TOC.

3. Results and discussion

3.1. Synergetic degradation of quinoline in saline water

Measured quinoline concentrations were decreased rapidly in the photoelectrocatalytic reactor with increasing reaction time, as indicated by the gently decreasing HPLC peak for the single adsorption process and rapidly decreasing HPLC peaks for the other processes (Fig. 3). The peak

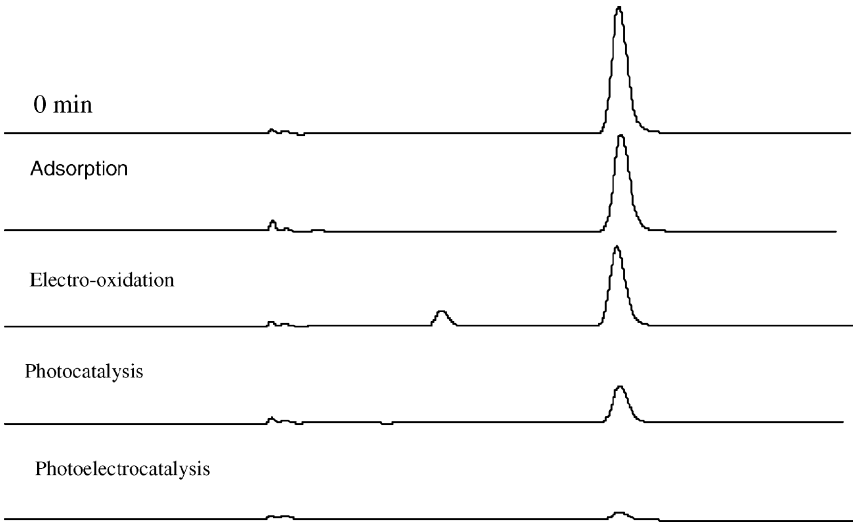

Fig. 3. HPLC spectra comparison of quinoline degradation by photocatalysis, electro-oxidation, photoelectrocatalysis and adsorption (reaction time: 120 min).

areas of quinoline remaining in the solution by photocatalytic, electrochemical and adsorption process were 4.4, 9.4 and 11.7 times, respectively of that by photoelectrocatalytic process at 120 min, which indicated that the degradation of quinoline by the photoelectrocatalytic process was more efficient than the photocatalytic or electrochemical process alone.

The progression of quinoline degradation indicated that quinoline could be removed from the solution by all four processes, and the profiles were presented in Fig. 4. However, only a 22% of quinoline was removed by adsorption of packed material at 120 min, compared to 71 and 38% removal of quinoline by the photocatalytic and electrochemical oxidation processes, respectively. These degradation efficiencies were all apparently lower than that of photoelectrocatalytic process (93%). When the adsorption effect was taken out from above three processes, 15, 49 and 71% of quinoline were degraded in the electrochemical oxidation, photocatalytic and photoelectrocatalytic processes, respectively. The net efficiency of the photoelectrocatalytic process was not only greater than that of photocatalytic or electrochemical process, but also greater than the sum of both processes. This enhancement effect of quinoline degradation may be evident of photoelectrocatalytic synergetic effect, which exists in the three-dimensional electrode-packed bed photocatalytic reactor.

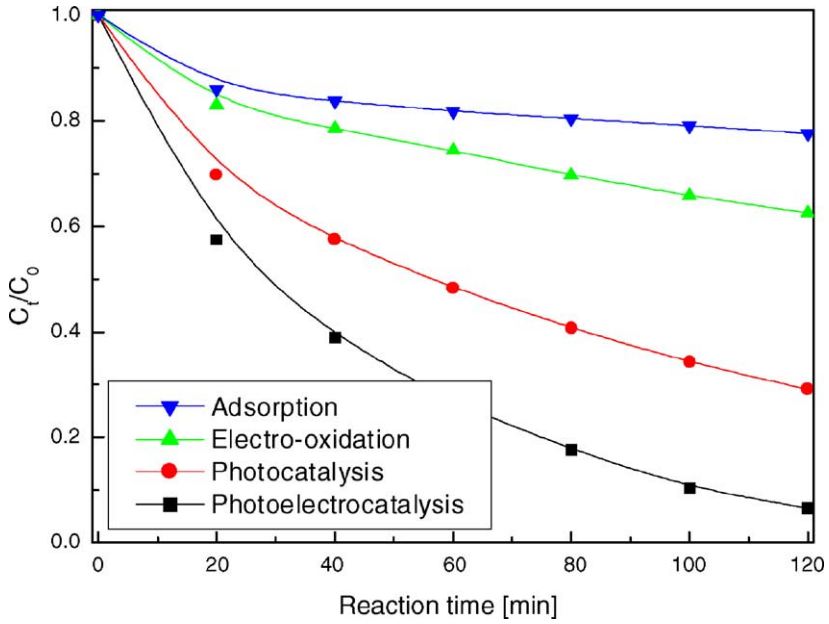

Fig. 4. Comparison of quinoline degradation efficiency.

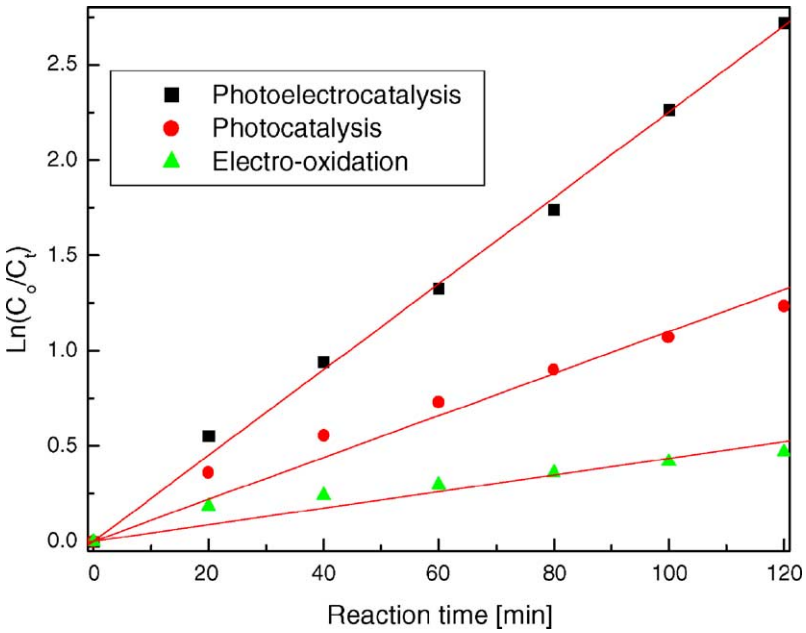

Fig. 5. Kinetics curves in the three processes.

In general, the dependence of the photocatalytic reaction rates on the concentration of organic pollutants has been described well by the Langmuir–Hinshelwood kinetic model, and the model can be simplified to a pseudo first-order equation [26]. In this work, photocatalytic degradation of quinoline fit well with the pseudo first-order equation. Moreover, the pseudo first-order kinetics was also confirmed in both the electrochemical process and the photoelectcrocatalytic process by expressing the data in Fig. 4 with $\ln(C_0/C_t) = k(t)$, and the kinetic curves were shown in Fig. 5. The apparent rate constants for the processes of photoelectrocatalysis, photocatalysis and electrochemistry were 0.0225, 0.0110 and 0.0044 min^{-1}, respectively. The rate constant of photoelectrocatalysis was 2.0 and 5.1 times of those in the photocatalytic and electrochemical processes, respectively. Therefore, an apparent synergetic effect in the degradation of quinoline was created in the photoelectrocatalytic reactor. According to the definition of synergetic effect (SF) $= Rpe - (Rp + Re)$ in our previous study [20], the SF obtained from the kinetic constants was 0.0071 min^{-1}. This further confirmed that an apparent kinetic synergetic effect was indeed observed in the photoelectcrocatalytic process.

The enhancement effect on photocatalytic process at high cell voltage may be attributed to two factors. First, external electric field can capture photogenerated electrons, reducing the recombination of these electrons and holes. Moreover, three-dimensional electrode with expanded specific areas has a greater collecting capacity of photo-generated electrons than those with holes, resulting in the improvement of photoelectrocatalytic process. Second, the external electric field can also result in the direct or indirect electrochemical oxidation of quinoline besides photoelectrocatalytic synergetic effect [20–22]. The reaction mechanism for the three-dimensional electrode assisted photocatalytic degradation of organic pollutants under electric field was discussed in our previous literatures [21,22], and the degradation mechanism is believed to involve many oxidation routines, such as anodic oxidation, oxidation of electrogenerated H_2O_2 and $OH^{\bullet}$, oxidation of photogenerated hole and $OH^{\bullet}$, and the photoelectrocatalytic synergetic effect, etc.

3.2. TOC reduction in the three processes

It has been known that the application of photocatalytic and photoelectrocatalytic processes can mineralize the toxic organic pollutants to inorganic materials or convert them to readily biodegradable intermediates. The kinetics of TOC reduction in the three processes (Fig. 6) showed that TOC

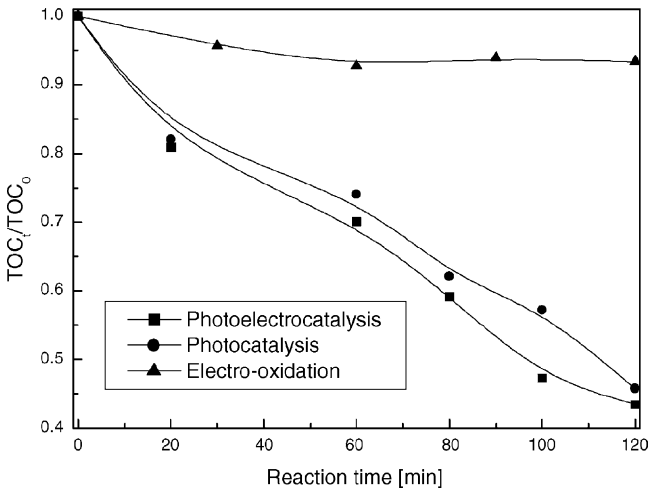

Fig. 6. TOC reduction during the degradation of quinoline.

reduction was much slower in the electrochemical process than those in the photocatalysis and photoelectrocatalysis processes, suggesting that electrochemical process was inefficient in the mineralization of quinoline. It can be seen that TOC reduction was faster in the photoelectrocatalytic process than that in the photocatalytic process, indicative of a small enhancement. The maximum TOC reduction reached 53 and 43%, respectively, for the photoelectrocatalytic and photocatalytic process at 100 min. Thus, we can conclude that in all three processes complete mineralization of quinoline to CO_2 was not accomplished directly; instead, it possibly proceeded via a number of intermediate steps. Complete understanding of the pathway and reaction mechanism for degradation of quinoline remains to be accomplished in future investigations.

3.3. Effect of Cl^- ion concentrations

Chloride ion, a very common inorganic ion frequently present in nature water or anthropogenic wastewater, has been found to be a scavenger for heterogenous photocatalytic process [23,27–31] by competing for surface active sites and forming weaker Cl radical [23]. In addition, Sunada et al. [32] mentioned that chloride ion could assist the recombination of photogenerated electrons and holes through a short-circuiting mechanism with which adsorbed chlorides were oxidized to adsorbed chlorine atoms by holes, and then reduced to chloride by electrons. On the other hand, NaCl was often used as supporting electrolyte for the photoelectrocatalytic degradation of organic contaminants [7,24,33]. In order to elucidate the effect of Cl^- ion and its concentrations on the photoelectrocatalytic degradation of quinoline, we used NaCl as an electrolyte in the new-designed photoelectrocatalytic reactor. The kinetic curves were presented in Fig. 7, and it is noted that the apparent rate constant was 0.0089 min^{-1} with no Cl^- ions added, but increased to 0.0327 min^{-1} when the concentration of Cl^- ions reached 1.0 mol l^{-1}. It is interesting to note that chloride ions had an obvious enhancement effect rather than a scavenging effect on the degradation of quinoline in this photoelectrocatalytic reactor when NaCl was used as supporting electrolyte.

The enhancement can be interpreted as follows. At low Cl^- ion concentrations, Cl^- ion competed for oxidizing radicals or active sites of the catalyst, resulting in some extent of scavenging effects associated with the photoelectrocatalytic degradation of quinoline. However, with the increase of Cl^- ions concentration the adsorption of Cl^- ions reached equilibrium. As a result, the surplus free Cl^- ions as electrolytes could enhance charge-transfer in the photoelectrocatalytic reactor, leading to an increase in capture effects for photogenerated electrons under external electric field. Moreover, increase in electrolyte concentration could lead to a large increase in the efficiency of quinoline degradation by direct and/or indirect electrochemical oxidation under high cell voltage. In addition, Cl_2 and other active species, formed by direct or indirect electrochemical reaction from Cl^- ion in the photoelectrocatalytic reactor, could also assist the photocatalytic degradation of quinoline.

3.4. Effect of cell voltage

To increase the photocatalytic efficiency of semiconductors for degrading undesirable organics in aqueous solution, the anodic bias was also used for nanocrystal semiconductor photocatalysis [9,15,16]. Fujishima and Honda [34] first used a single-crystal rutile TiO_2 photoanode for photoelectrochemical decomposition of water under the influence of an anodic bias. However, in the electrochemically assisted

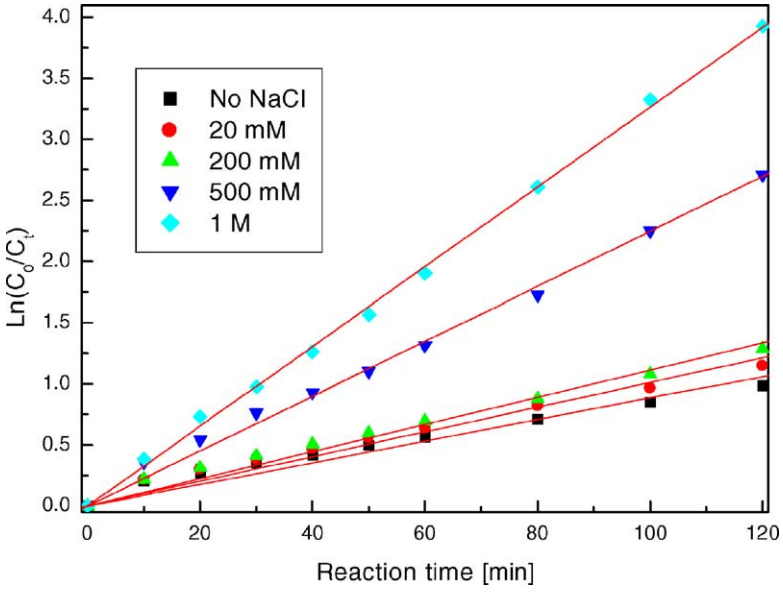

Fig. 7. Effect of Cl^- ion concentration on the rate constant.

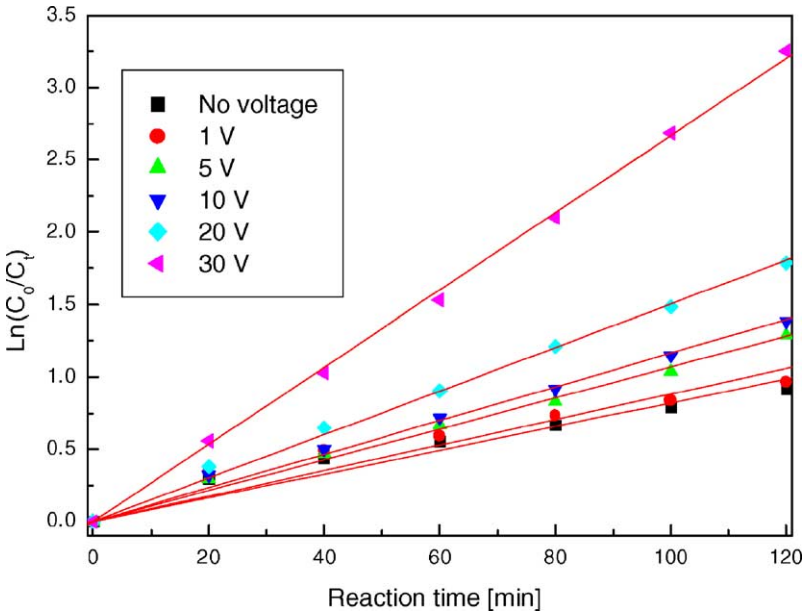

Fig. 8. Effect of applied cell voltage (quinoline concentration: 0.5 mmol l^{-1}).

photocatalytic experiments, the applied anodic bias potential is always lower than that of objective organic pollutant so that no direct electrochemical oxidation complicates the photocatalysis [9,15,16]. However, the cell voltage in the photocatalytic degradation of organic pollutants not only is able to depress the electron-hole recombination, but also provides the capability for direct or indirect electrochemical oxidation of the organic pollutants, especially in the case of the three-dimensional electrode technology [21,22]. Thus, we investigated the effect of electric field on the photoelectrocatalytic degradation of quinoline in saline water at cell voltages ranging from 0 to 30 V, and the results were illustrated in Fig. 8. The apparent rate constant increased slightly at low cell voltages but rapidly at cell voltages above 10 V. For example, the apparent rate constant was only 0.0082 min^{-1} without any cell voltage applied, and increased up to 0.0267 min^{-1} at 30 V cell voltage. The apparent rate constant increased by 3.3 times when 30 V cell voltage was applied to photocatalytic degradation of quinoline. This means that the cell voltage is a key parameter not only for the three-dimensional electrode technology, but also for the photoelectrocatalytic process.

This enhancement effect in the photoelectrocatalytic process may be attributed to both the capturing effect and direct oxidation by external electric field, i.e. the cell voltage has versatile effects on photocatalytic reaction. It not only can speed the degradation rate of organic pollutants, but also may change the degradation mechanism of organics in the photoelectrocatalytic reactor [8,9].

3.5. Effect of airflow

In general, a bubble column reactor with a porous plate distributor can offer best gas–liquid mass transfer efficiency [35]. In view of this consideration, a special kind of porous titanium plate was used as a gas distributor in this study. A SEM micrograph of the titanium plate surface shows that the plate was rather regular and porous (Fig. 9). It can be seen from Fig. 10 that many thinly distributed air-bubbles with a size of about 1 mm were generated in the reactor, which was beneficial to mass transfer and oxygen dissolving. It is well known that molecular oxygen plays an important role in the photocatalytic reaction and provides dual functions. One is to supply essential oxygen to capture photogenerated electrons, reducing the recombination of photogenerated electron and hole [36], and the other is to agitate the solution in order to speed up mass transfer [37].

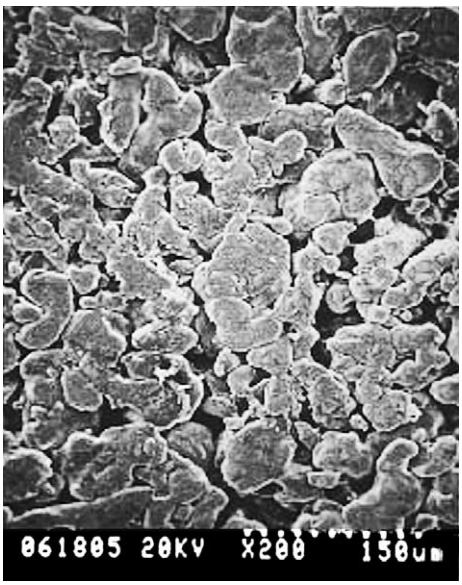

Fig. 9. SEM image of micropore titanium plate.

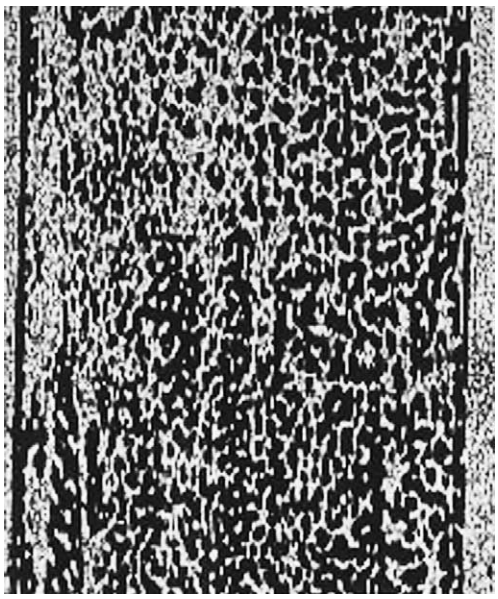

Fig. 10. Photograph of air bubble in the reactor.

Although the use of anodic bias obviates the need of oxygen as an electron acceptor in photoelectrocatalytic process, the presence of molecular oxygen still show a positive effect on both the rate and the degradation pathways of organic pollutants [8,9]. That is, molecular oxygen plays an important role in the photocatalytic and photoelectrocatalytic degradation of the organic pollutants. In the present study, the compressed air was sparged into the photoelectrocatalytic reactor from the bottom of the reactor through porous titanium plate in all the experiments.

The relationship between airflow and the rate constant of photoelectrocatalytic degradation of quinoline was presented in Fig. 11. It is obvious that the rate constants increased considerably from 0.0118 to 0.0204 min^{-1} with increasing air flow, but exhibited a maximum at approximately 0.05 MPa and then decreased slightly after this value. This may be due to the fact that the adsorption reaction of quinoline onto the catalyst could be considerably slowed when more air was sparged into the reactor. Additionally, the capturing effect of molecular oxygen to photogenerated electrons also could be greatly reduced because large airflow was not favorable to the adsorption of air onto the photocatalyst.

3.6. Effect of pH value

For charged substrates, pH value has a significant effect on photocatalytic degradation of organic pollutants while the effect is rather insignificant for photocatalytic degradation of neutral substrate [38]. Quinoline is a weak organic tertiary amine base, and it may be presented in different forms depending on the pH value in the solution. Therefore, the pH value would have a significant effect on the adsorption–desorption properties of quinoline at the catalyst's surface and might be an important parameter in photoelectrocatalytic and photocatalytic degradation of quinoline.

The relationship between pH value and the rate constants of photoelectrocatalytic degradation of quinoline in the reactor was shown in Fig. 12. Degradation rate for quinoline increased rapidly with an initial increase of pH value, but decreased slightly after pH value reached ~10. Specifically, the apparent rate constant increased by 5.6 times from 0.0136 min^{-1} at pH 2.04 to 0.0760 min^{-1} at pH 9.06. Two disadvantageous effects existed in solution with the increase of solution pH [39], but Beltran et al. [40] thought that the scavenging effect became stronger until the pH value was higher than 11.8, pK_a of hydrogen peroxide dissociation

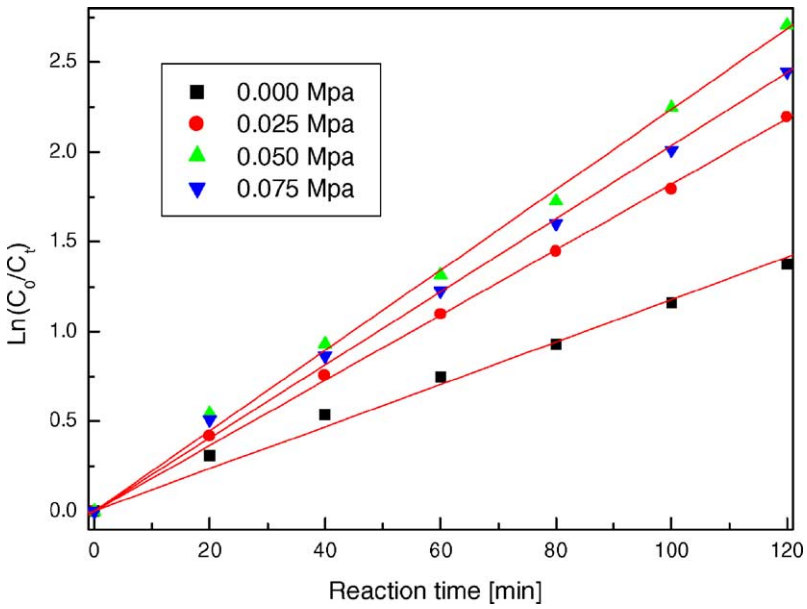

Fig. 11. Effect of airflow on the rate constant.

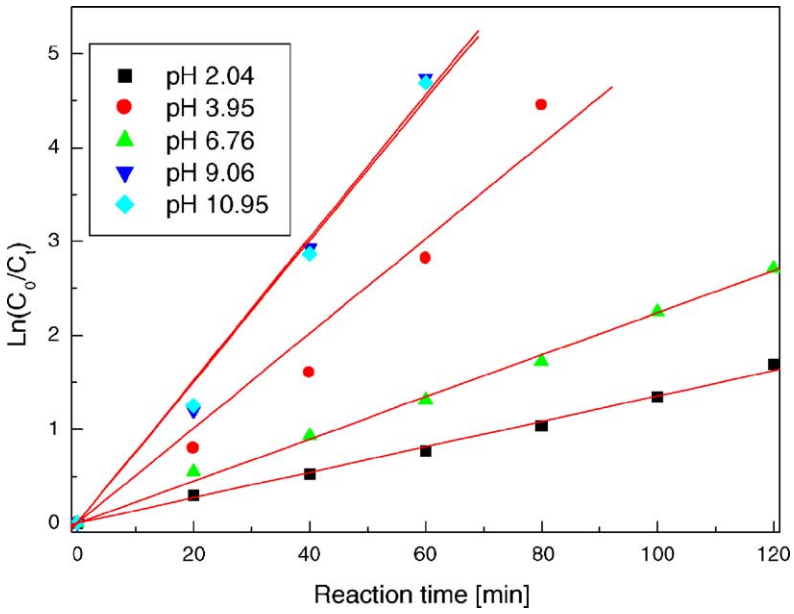

Fig. 12. Effect of pH value on the rate constant.

equilibrium constant. Thus, it is plausible that the rate constant of the degradation of quinoline increased rapidly with the increase of pH value in the present study, and the photoelectrocatalytic degradation of quinoline was more favorable in alkali solution than in acidic solution. This is due to the fact that at low pH values, quinoline molecules presented in the protonated form with a positive charge cannot easily be adsorbed onto the surface of TiO_2 also with positive charges. When the pH value is larger than 6, the surface of TiO_2 gradually becomes negatively charged, and the adsorption of quinoline onto TiO_2 becomes much easier than that at low pH values. Another reason is that high pH values have been found to be favorable for the formation of hydroxyl radical from the direct photolysis of hydrogen peroxide since the extinction coefficiency of ionic form of hydrogen peroxides, the hydroperoxide ions (major peroxide species at alkali conditions), was higher than that of the nonionic form at 254 nm.

Acknowledgements

This work was financial support from the State laboratory Innovation Base Foundation (001108), and the Opening Project of State Key Laboratory of Organic Geochemistry (OGL-200210).

References

[1] A.K. Ray, Catal. Today 44 (1998) 375.
[2] C.M. Wang, H. Adam, G. Heinz, J. Am. Chem. Soc. 114 (1992) 5230.
[3] K. Takeda, K. Fujiwara, Water Res. 30 (1996) 323.
[4] W. Choi, A. Termin, M.R. Hoffmann, J. Phys. Chem. 98 (1994) 13669.
[5] C. Wang, J.C. Zhao, X.M. Wang, B.X. Mai, P.A. Peng, G.Y. Sheng, J.M. Fu, Appl. Catal. B: Environ. 39 (2002) 269.
[6] Y.R. Do, J. Solid State Chem. 108 (1994) 198.
[7] R.J. Candal, W.A. Zeltner, M.A. Anderson, J. Adv. Oxid. Technol. 3 (1998) 270.
[8] K. Vinodgopal, U. Stafford, K.A. Gray, P.V. Kamat, J. Phys. Chem. 98 (1994) 6797.
[9] K. Vinodgopal, E.E. Wynkoop, P.V. Kamat, Environ. Sci. Technol. 30 (1996) 1660.
[10] R. Pelegrini, P. Peralta-Zamora, A.R. Andrade, J. Reyes, N. Duran, Appl. Catal. B: Environ. 22 (1999) 83.
[11] J. Rodriguez, M. Gomez, S.E. Lindquist, Thin Solid Films 360 (2000) 250.
[12] T.C. An, C. He, X.H. Zhu, H.F. Gu, Chin. J. Catal. 22 (2001) 231.
[13] S.A. Walker, P.A. Christensen, K.E. Shaw, J. Electroanal. Chem. 393 (1995) 137.
[14] I.M. Butterfield, P.A. Christensen, A. Hamnett, K.E. Shaw, G.M. Walker, S.A. Walker, C.R. Howarth, J. Appl. Electrochem. 27 (1997) 385.
[15] K. Vinodgopal, S. Hotchandani, P.V. Kamat, J. Phys. Chem. 97 (1993) 9040.
[16] J.M. Kesselman, N.S. Lewis, M.R. Hoffmann, Environ. Sci. Technol. 31 (1997) 2298.
[17] J.O. Bockris, J. Kim, J. Appl. Electrochem. 27 (1997) 890.
[18] K. Rajeshwar, J.G. Ibanez, M. Swain, J. Appl. Electrochem. 24 (1994) 1077.
[19] E. Brillas, R. Sauleda, J. Casado, J. Electrochem. Soc. 144 (1997) 2374.
[20] T.C. An, Y. Xiong, G.Y. Li, C.H. Zha, X.H. Zhu, J. Photochem. Photobiol. A: Chem. 152 (2002) 155.
[21] T.C. An, X.H. Zhu, Y. Xiong, J. Environ. Sci. Health. 36A (2001) 2069.
[22] T.C. An, X.H. Zhu, Y. Xiong, Chemosphere 46 (2002) 897.
[23] R.A. Burns, J.C. Crittenden, D.W. Hand, V.H. Selzer, L.L. Sutter, S.R. Salman, J. Environ. Eng. 125 (1999) 77.
[24] D.H. Kim, M.A. Anderson, Environ. Sci. Technol. 28 (1994) 479.
[25] Y. Xiong, T.C. An, X.H. Zhu, J. Appl. Geochem. in press.
[26] D.F. Ollis, Environ. Sci. Technol. 19 (1985) 480.
[27] M. Abdullah, G.K. Low, R.W. Matthews, J. Phys. Chem. 94 (1990) 6820.

[28] H.Y. Chen, O. Zahraa, M. Bouchy, J. Photochem. Photobiol. A: Chem. 108 (1997) 37.
[29] A. Piscopo, D. Robert, J.V. Weber, Appl. Catal. B: Environ. 35 (2001) 117.
[30] M. Sokmen, A. Ozkan, J. Photochem. Photobio. A: Chem. 147 (2002) 77.
[31] K.H. Wang, Y.H. Hsieh, C.H. Wu, C.Y. Chang, Chemosphere 40 (2000) 389.
[32] P. Sunada, A. Heller, Environ. Sci. Technol. 32 (1998) 282.
[33] R.J. Candal, W.A. Zeltner, M.A. Anderson, Environ. Sci. Technol. 34 (2000) 3443.
[34] A. Fujishima, K. Honda, Nature 238 (1972) 37.
[35] J. Lea, A.A. Adesina, J. Photochem. Photobiol. A: Chem. 118 (1998) 111.
[36] G.H. Huang, B. Marinas, Environ. Sci. Technol. 31 (1997) 562.
[37] I.Z. Shirgaonkar, A.B. Pandit, Ultrason. Sonochem. 5 (1998) 53.
[38] I. Arslan, I.A. Balcioglu, D.W. Bahnmann, Appl. Catal. B: Environ. 26 (2000) 193.
[39] C.H. Liao, D.G. Mirat, Environ. Sci. Technol. 29 (1995) 3007.
[40] F.J. Beltran, G. Ovejero, J. Rivas, Ind. Eng. Chem. Res. 35 (1996) 883.